Astron. Astrophys. 336, 823–828 (1998)

ASTRONOMY
AND
ASTROPHYSICS

Hot dust in the active nucleus of NGC 7469 probed by adaptive optics observations⋆

O. Marco[1] **and D. Alloin**[2]

[1] Observatoire de Paris, DESPA (URA CNRS 264), F-92195 Meudon, France
[2] Service d'Astrophysique, CE Saclay (URA CNRS 2052), F-91191 Gif-sur-Yvette, France

Received 8 July 1997 / Accepted 27 March 1998

Abstract. The use of adaptive optics has allowed to reach in the infrared an angular resolution around 0.35", allowing to study the temperature, mass and distribution of the dust component within the 400 pc radius central region of NGC 7469. We have obtained L and L' band images which show an unresolved core (r<55 pc) embedded in an extended emission component. Not to mention the ring of star formation, known to be present at r∼1.5", which cannot be studied from this data set because of its quite low surface brightness and will not be discussed here. We find that about 55% of the 3.5 and 3.8 μm flux across the 1.4"×1.4" central region arises from the unresolved core. The hot and warm dust grain density in the extended component follows an $r^{-1.5}$ law, and the dust temperature ranges from 900 K (r∼130 pc) to ∼300 K (r∼400 pc). The mass of hot (T=900 K) dust within a r∼200 pc central region is ∼0.05 $M_\odot$ and it accounts for 36% of the 2.2 μm emission in this region.

These results are in good agreement with a composite model of active nucleus including a parsec scale dusty torus surrounded by an extended hot dust region located in the NLR and heated by the central engine.

Key words: galaxies: individual: NGC 7469 – galaxies: Seyfert – galaxies: nuclei – infrared: galaxies

1. Introduction

Series of observational facts assembled over the past decade on Active Galactic Nuclei have led to the so-called "unified" model of AGN (for a review of these facts, as well as for the detailed characteristics of the unified model see e.g. Antonucci, 1992).

Our specific interest in the unified model is that the central engine (black hole and accretion disk or compact starburst region) and its close environment (dense gas clouds emitting the broad lines which constitute the broad line region, BLR) are embedded within an optically thick dusty/molecular torus. Along some lines of sight, the torus may obscure and even fully hide the central engine and BLR.

As a straightforward conclusion, we are naturally led to search for the torus through its infrared emission, which, according to current models should be quite strong (Pier & Krolik, 1992b ; Efstathiou & Rowan-Robinson, 1995 ; Granato & Danese, 1994 ; Granato et al., 1996, 1997): the near-infrared spectral energy distribution of most AGN shows a bump peaking at 3-5 μm (Edelson & Malkan, 1986 ; Robson et al., 1986), and a torus with a mean dust temperature of T∼800 K would give rise to a peak in the L band (3.5 μm). In this search, high spatial resolution is imperative in order to locate very precisely the torus emission: hence, adaptive optics in the 1-5 μm window is the tool.

As a bright Seyfert 1 galaxy, NGC 7469 is well suited for the study of the dust component. Its proximity, 66 Mpc (H_0=75 km/s/Mpc), its brightness (m_v≈13 for the unresolved core used by the wavefront analysis sensor) allows to observe it with an adaptive optics system at a resolution down to 110 pc (0.35") at 3.8 μm. Observations had been made previously in the near-infrared 1-2.2 μm (Genzel et al., 1995), analysing the nuclear gas and the 500 pc radius starburst ring. In the current study, we are presenting new results obtained with adaptive optics at 3.5 and 3.8 μm, with a special attention to the very central source (r<1.4").

2. Observations and data reduction

We observed the central region of NGC 7469 at 3.48, 3.81 and 4.83 μm with ADONIS, the adaptive optics system installed at the ESO 3.60-meter telescope (La Silla, Chile). The adaptive optics system is fully described in Beuzit et al. (1994). The ADONIS system was equipped with the COMIC camera, working from 3 to 5 μm. The wavefront was directly sensed on the bright visible nucleus of NGC 7469 and the adaptive optics correction on the nucleus was performed in the infrared.

The observations were made on August 17, 1996, under excellent seeing and transparency conditions (seeing ∼0.6"), as indicated in Table 1.

We used the COMIC camera (Bonaccini et al., 1996), at the f/45 Cassegrain focus, which provides an image scale of 0.1"/pixel, resulting in a field of view of 12.8" × 12.8". The COMIC detector is a 128×128 HgCdTe photovoltaic focal plane array. At 77 K, the average dark current is 2000 e^-/sec and

Send offprint requests to: O. Marco

⋆ Based on observations collected at the European Southern Observatory, La Silla, Chile.

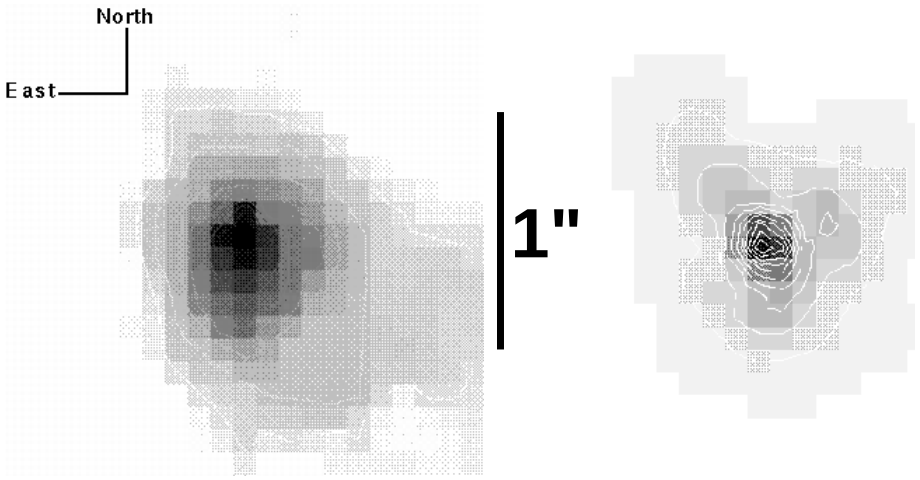

Fig. 1. Left: L band image of NGC 7469. Right: PSF from a nearby star

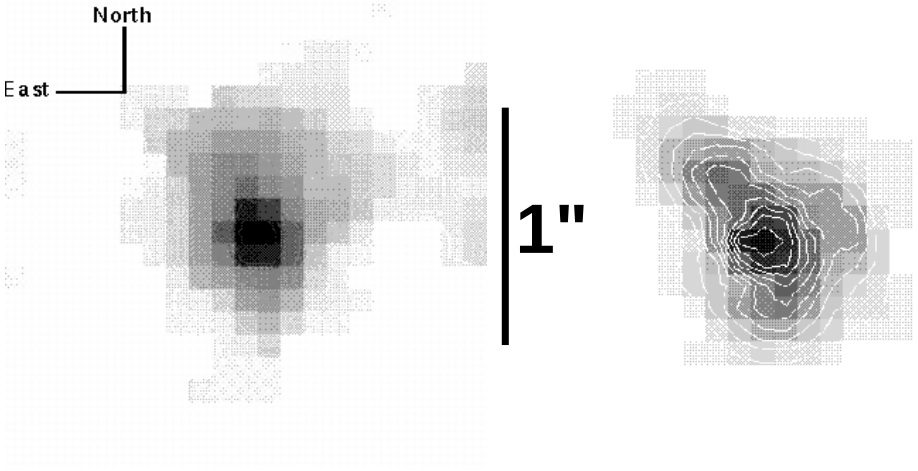

Fig. 2. Left: L' band image of NGC 7469. Right: PSF from a nearby star

the total capacity is about $6\,10^6$ electrons. The readout noise is about 1000 e^- *rms* allowing to observe under conditions of background limiting performances (BLIP) for individual exposure times larger than 500, 260 and 150 ms for the L, L' and M bands respectively (Lacombe et al., 1997). In this way, the readout-noise is dominated by the background photon noise, and we just take a mean of a series of individual images to improve the signal-to-noise ratio.

For the L, L', and M bands, we observed in a chopping mode, alternating object and sky images by the use of a field selection mirror. We chose an offset of 10" to the north and 10" to the west.

We observed several photometric standard stars to obtain a good calibration in flux, and another star to determine the point spread function (PSF) for deconvolution.

Standard infrared data reduction procedures were applied to each individual frame, for both the galaxy and the reference stars : dead pixel removal, sky subtraction, flat fielding. We payed careful attention to flatfielding, spending several hours at the start or at the end of the nights, to record sky images and to derive an excellent flatfield for each wavelength. The adaptive optics system compensates for image shifting. We cross-correlated individual images to track residual shifts: the centroid coincidence between individual frames was found to be always better than 1 pixel (i.e. 0.05"). So no additional shift correction had to be applied.

3. Data analysis

We present in Figs. 1 and 2 the L and L' band images of NGC 7469. We have also observed NGC 7469 in the M band, but it has not been detected, most probably because of the low sensitivity of the infrared detector. Thus, our current data analysis will be based on the two bands L and L'.

The L and L' images show an unresolved core down to the resolution of 0.4" (130 pc) and 0.35" (110 pc) respectively, surrounded by an extended emission component, ($r \leq 400$ pc), which does not appear as a ring like structure and could not be related to the starburst ring (Wilson et al., 1991, Mauder et al., 1994, Genzel et al., 1995), located farther away ($r \geq 480$ pc, $r \geq 1.5$"). Thus, in the following, we leave aside the analysis of the starburst ring which could not be detected during our observations because of too short integration times and we concentrate on the discussion of the innermost 1.4"$\times$1.4".

So far, the exact performances of adaptive optics when using a faint reference for the wavefront analysis sensor have not been fully explored. Especially in the case of a slightly extended ref-

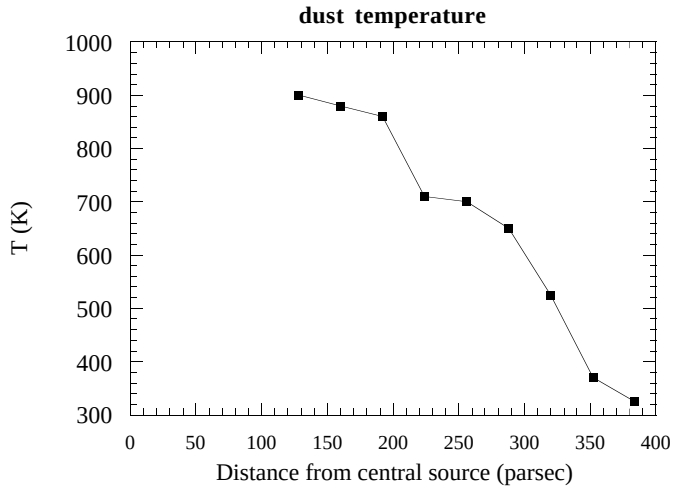

Fig. 3. Dust temperature as a function of distance from the central source

Table 1. Summary of the data sets

filter	λ	$\Delta\lambda$	T_{int}	T_{total}	FWHM	seeing	airmass
L	3.48 μm	0.59 μm	7.0 s	448 s	0.40"	$\sim$0.6"	1.30
L'	3.81 μm	0.62 μm	3.5 s	336 s	0.35"	$\sim$0.6"	1.27

Table 2. Photometric data for NGC 7469

filter	λ	aperture	flux	author
K	2.2 μm	1.4"	60 ± 6 mJy	Genzel et al., 1995
L	3.5 μm	1.4"	125 ± 13 mJy	this paper
L'	3.8 μm	1.4"	145 ± 15 mJy	this paper
PAH	3.3 μm	2"	8 mJy	Mazzarella et al., 1994
mid IR	8-13 μm	4.6"	1080 ± 10 mJy	Miles et al., 1996

erence, there might be a slight residual astigmatism (Appendix A). In the case of NGC 7469, however, the visible nucleus is observed to be point-like and this effect is fully negligible. We ignore it hereafter.

However, to prevent any spurious effects due to the use of a PSF (from a nearby star) possibly not exactly identical to that corresponding to the NGC 7469 data, we chose not to apply any deconvolution process on the images. Measurements in the following analysis are based upon the cleaned (sky-subtracted, dead pixels removed, flat-fielded) images only.

4. Flux measurements

Fluxes have been measured on the reduced images (not deconvolved). They have been measured simulating a circular aperture with a radius varying from 4 to 12 pixels (128 to 384 pc). In Table 2, we summarize these measurements, together with measurements in others wavebands. We note that the PAH line emission at 3.3 μm contributes at most $\sim$6% of the flux in the L band.

The L and L' band apertures have been centered on the peak of the corresponding flux distributions and it was assumed that the peak of the K-band flux distribution is coincident with these peaks.

This assumption implies that the central source is the hotest component in the AGN of NGC 7469, heating the surrounding dust, and thus is the brightest source at 2.2, 3.5 and 3.8 μm.

Due to the adaptive optics system, the infrared camera field has a position fixed in regard to the centroid of the visible counterpart of the object observed. Observing a star, we determine the infrared image reference position, which corresponds to the visible reference position (for a star, the infrared and optical peaks are coincident). Any offset of the galaxy infrared peak relatively to the star infrared peak would correspond to a real offset between the galaxy infrared peak and its visible peak. This gives an indication for the positioning of the infrared with respect to visible sources, in the AGN.

For a type 1 AGN, models suggest that we observe a face-on nucleus: then, the torus center should correspond to both the optical and infrared emission peaks. We find that the NGC 7469 L (and L') band peak is offset by 0.2 ± 0.1" north of the visible continuum peak. Down to the achieved spatial resolution (0.35") this shift is not significant. The coincidence between the visible and L band peaks in NGC 7469 hence indicates that the nucleus is indeed seen face-on, in contrary to the the case of NGC 1068, a type 2 AGN, where we find an offset between the infrared and the optical peaks of $\sim$0.3" (Marco et al., 1997) suggesting that the nucleus is viewed at a large inclination angle.

We have estimated the fraction of unresolved flux in the L (and L') band images, by normalizing the PSF to the same peak surface brightness as the galaxy and taking the ratio of the total normalized PSF flux to the total galaxy flux.

The flux in the unresolved core (r<55 pc) accounts for at least 55% of the total flux, and therefore is about 1.2 times the flux of the extended source possibly related to the narrow line region (NLR) dust. Miles et al. (1996) give a value of 60% in the mid-IR ($\sim$10 μm) for the fraction of unresolved flux. The spatial resolution of their data is around 0.6", which prevents us to perform a direct comparison with the flux prediction at 10 μm from the unresolved dust component measured at 3.5 μm and 3.8 μm with an angular resolution of $\sim$0.4". However, we can check these two estimates in terms of their relative values: we predict that the unresolved (r<0.4") dust component detected at 3.5 and 3.8 μm, with a temperature of 900 K, should radiate around 130 ± 50 mJy at 10 μm. This is indeed smaller than the observed 650 mJy emission measured by Miles et al. (1996) from their unresolved source (r<0.65").

What is the nature of the unresolved core ? It could be related to a compact dust/molecular thick torus like in the unified models by Pier & Krolik (1992a, 1992b), Efstathiou & Rowan-Robinson (1995), Granato & Danese (1994), Granato et al. (1996, 1997), or result from emission by hot dust (T>900 K) mixed with gas in the NLR/BLR interface, and shielded from the intense UV radiation field.

5. Dust temperature

Based on the flux measurements, we can deduce a blackbody temperature from the L to L' ratio. These two bands are not the best choice for this, being close in wavelength, however, we recall that we did not detect NGC 7469 in the M band. We have estimated the measurement error on the flux to be 10%, which leads to an error on the temperature of $\pm$200 K.

Thanks to the high angular resolution achieved in the L and L' band images, we were also able to derive the dust temperature at increasing distances from the central source of the AGN. These results are presented in Fig. 3. The temperature decreases (from $\sim$900 K to $\sim$300 K) when the dust emission originates further away from the central source of the AGN (from $r\sim$130 pc to $r\sim$400 pc), suggesting that the central source is indeed responsible for the dust heating: heating by local sources (like starbursts) would lead to a more clumpy distribution in the dust temperature map.

Because the resolution is limited to $\sim$110 pc, we could not derive the dust temperature close to the central source ($r<$110 pc), and the highest value of 900 K is therefore a mean value over a 130 pc radius region. This means that nearer to the central source, the temperature is probably higher. How high could the temperature be ? This answer depends on the dust composition. The sublimation temperature of dust grains is above 1500 K for graphite, 1200 K for silicates and 1000 K for PAH. Because they can survive in quite strong UV radiation field, graphite and/or silicates are more probable. By extrapolating the temperature curve, we find that the dust temperature at $\sim$15 pc from the central source could be as high than 1250 K, excluding the presence of PAH very close to the central engine. The PAH emission measured by Mazzarella et al. (1994) within a 2" diaphragm must be therefore in a ring like configuration.

A temperature above 1250 K for the inner dust is expected in torus models to explain the observed spectral energy distribution (Granato & Danese, 1994). In particular, the nuclear optical and IR fluxes show clear evidence for a 1 μm minimum (Sanders et al., 1989), which can be explained by dust heated to its sublimation temperature $T_s\sim$1500 K (Granato & Danese, 1994). With regard to dust temperature, our observations favor this interpretation.

The K band flux from Genzel et al. (1995) is given for a 1.4" diameter aperture. We have computed the corresponding flux in the L and L' bands for a 1.4" diameter aperture. Fitting the L and L' fluxes with a blackbody emission, we find a mean temperature of 900 K for this region. We then derive the K band flux corresponding to this blackbody emission. We find that the K band flux contributed by the dust component in this region must be 22 ± 2 mJy. Genzel et al. (1995) give a value of 60 ± 6 mJy for the K band flux, showing therefore that the hot dust component accounts for 36$\pm$3% of the near-infrared flux in a $r\leq$225 pc region around the central source of the AGN. Based on the visible/infrared spectral energy distribution, Genzel et al. (1995) calculate that about one third to half of the K-band flux might be stellar. This suggests that the rest of the near-infrared flux (from 14% to 34%) is related to a non-thermal emission from the central engine.

6. Dust mass

The mass of dust associated with the near-infrared emission can be only roughly estimated, because it depends on the (unknown) grain sizes and composition. Assuming graphite grains and following Barvainis (1987), the infrared spectral luminosity of an individual graphite grain is given by:

$$L^{\rm gr}_{\nu,{\rm ir}} = 4\pi a^2 \pi Q_\nu B_\nu(T_{\rm gr}) \ {\rm ergs\,s^{-1}\,Hz^{-1}}$$

where a is the grain radius, $Q_\nu = q_{\rm ir}\ \nu^\gamma$ is the absorption efficiency of the grains, and $B_\nu(T_{\rm gr})$ is the Planck function for a grain temperature $T_{\rm gr}$. Following Barvainis (1987), we take a=0.05 μm and Q_ν=0.058. With $T_{\rm gr}$=900 K, we find $L^{\rm gr}_\nu = 1.49\,10^{-18}$ ergs s^{-1} Hz^{-1}.

In NGC 7469 the K band flux is F_ν=2.2 10^{-25} ergs s^{-1} cm^{-2} Hz^{-1}, at a distance D=66 Mpc. We derive the number of hot ($T_{\rm gr}$=900 K) grains: n=7.58 10^{46}. Taking a grain density ρ=2.26 g cm^{-3}, we get: M(hot dust)$\sim$0.05 $M_\odot$. This result is comparable to the 0.02 $M_\odot$ mass of hot dust found in another Seyfert 1 nucleus, Fairall 9 (Clavel et al., 1989), but substantially larger than in other AGN: 2.5 $10^{-3} M_\odot$ in NGC 3783 (Glass, 1992), 7 $10^{-4} M_\odot$ in NGC 1566 (Baribaud et al., 1992) and 5 $10^{-4} M_\odot$ in NGC 4593 (Santos-Lléo et al., 1995).

7. Spatial distribution of the dust

In NGC 7469, dust is present also in the NLR region. We have derived the distribution in the number of dust grains over the nuclear region, from $r\sim$200 pc to $r\sim$400 pc of the central source of the AGN, with a temperature ranging from 900 K to 300 K (Fig. 4). We note that this number increases regularly with distance from the central source.

We have also computed the grain density as a function of distance from the central source (Fig. 4). Fitting this distribution by a power law, we find that the hot and warm dust grain density follows an $r^{-1.5}$ distribution.

8. Comparison with thick tori model predictions

Several torus models have been developped so far to explain the obscuration of the BLR and UV/X-ray continuum sources from some lines of sight (AGN unification scheme).

Pier & Krolik (1992a, 1992b, 1993) propose a thick parsec scale uniform density annular ring of dust, illuminated by a central point source. The dust can be heated up to T$_{eff}$, the effective temperature of the nuclear radiation on the inner edge of the torus. They investigate models with 500 K$<$T$_{eff}$ $<$2000 K. This kind of model could explain the unresolved core observed in NGC 7469. What about the emission of the extended dust component ? In the case of NGC 1068, a bright Seyfert 2 nucleus, these authors explain the 1"-2" extended infrared emission partly by reflected radiation from the torus and partly by

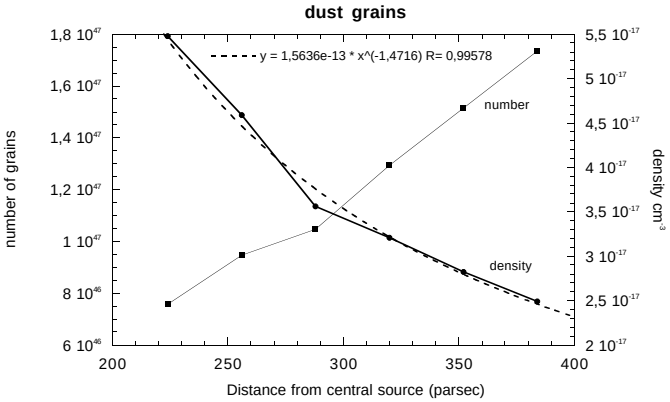

Fig. 4. Number and density of dust grains as a function of distance from the central source

dust in the NLR. In the case of NGC 7469 this interpretation seems difficult to conciliate with our observations, because the dust temperature is shown to decrease monotonically with the distance from the central engine, suggesting the latter to be responsible for the dust heating.

Efstathiou & Rowan-Robinson (1995) propose a model with a very thick tapered disk following a r^{-1} density distribution. They assume the melting temperature of all dust grains to be identical (1000 K), but they note that the radius at which each grain type in the mixture reaches this temperature is different. In the case of NGC 1068, Efstathiou et al. (1995) have shown that the torus emission alone cannot account for the entire infrared emission. They attribute the excess infrared emission to a component of optically thin dust distributed as r^{-2} within the NLR region. This model could apply as well in the case of NGC 7469, as we observe an unresolved core and an extended, temperature-decreasing component.

Granato & Danese (1994) and Granato et al. (1996, 1997) developped a simple thick (τ_e >30) torus model extended over several hundreds of parsecs. To keep the number of free model parameters to a minimum, they have adopted a dust density distribution constant with radial distance from the central source. This choice is clearly not compatible with our observations in the case of NGC 7469. Nevertheless, they do not rule out the possibility, in case of smaller values of optical depth (τ_e=1.5), that a more concentrated density distribution would be needed (following a $r^{-0.7}$ density distribution).

9. Conclusion

The use of adaptive optics has allowed to reach in the infrared the high angular resolution required to study the temperature, mass and distribution of the dust component in NGC 7469.

The mass of hot (T=900 K) dust surrounding the central source of the AGN, $\sim$0.05 $M_\odot$, is comparable to the mass of hot dust found in another Seyfert 1 galaxy, Fairall 9, although larger than in other AGN of lower intrinsic luminosity (NGC 3783, NGC 1566, NGC 4593).

The fact that about 55% of the infrared flux arises from an unresolved core, that the dust density is as $r^{-1.5}$, and that its temperature decreases when dust emission originates further away from the central source, (from 900 K at $r\sim$130 pc to $\sim$300 K at $r\sim$400 pc), have been faced with current torus models. It seems that the model developped by Efstathiou & Rowan-Robinson (1995) and Efstathiou et al. (1995) gives the best agreement with our observations of NGC 7469, but further modeling is desirable.

Acknowledgements. We are gratefully indebted to the ESO staff at La Silla, particularly P. Prado, for assistance during the adaptive optics observations. We warmly thank as well D. Bonaccini, E. Gendron, F. Lacombe and J.P. Veran for useful discussions.

Appendix A: about eventual residual astigmatism on the corrected images

The wavefront analysis sensor (WFAS) is divided into several microlenses. Each microlens is coupled with 8×8 pixels of an intensified CCD working in the visible. The WFAS takes the light gravity center over the 64 pixels, for each microlens. The microlenses are squared, while the pixels are rectangular. Because of this slight mismatch in shape, the microlens area is smaller than the corresponding pixels area.

The reference position for the WFAS is given by observing an optical fiber source. Since the microlens area and the pixel area are different, the reference position is not the pixel area center. During the observation, any offset between the reference and the current position is supposed to be due to atmospheric turbulence effects. This assumption is correct when one is looking at a point-like object. But if the wavefront analysis is performed on an extended object, the situation is more complex.

With an extended object like a galaxy, the pixels are fully illuminated, and the light gravity center is shifted in regard with a point-like source. This induces an astigmatism effect. This effect is not present on the PSF reference star, which is a point-like source for the WFAS. So, residual astigmatism cannot be removed while applying the deconvolution by the PSF. We have estimated the residual elongation due to this effect on NGC 7469: the images are not elongated at FWHM, but we find an elongation factor of 1.3 in the north-south axis, at 25% of maximum peak intensity. This residual effect is quite small and its impact on our measurements was minimized by avoiding to perform a PSF deconvolution and by deriving diaphragm-like fluxes.

However, a warning is given that one might have to take care of residual astigmatism when observing faint extended objects with ADONIS. This effect should be detectable on the WFAS control monitor during data acquisition. For a complete description of this effect, see Gendron et al. (1998).

References

Antonucci, R.R.J., 1992, in Testing the AGN Paradigm, eds. S.S. Holt, S.G. Neff, C.M. Urry (New York: AIP), AIP Conference Proceedings, Vol. 254, 486

Baribaud, T., Alloin, D., Glass, I., Pelat, D., 1992, A&A, 256, 375

Barvainis, R., 1987, ApJ, 320, 537

Beuzit, J.L., Hubin, N., Gendron, E., et al., 1994, SPIE 2201
Bonaccini, D., Lacombe, F., Marco, O., Eisenhauer, F., Hofmann, R., 1996, The Messenger, 82, 16
Clavel, J., Wamsteker, W., Glass, I.S., 1989, ApJ, 337, 236
Efstathiou, A., Rowan-Robinson, M., 1995, MNRAS, 273, 649
Efstathiou, A., Hough, J.H., Young, S., 1995, MNRAS, 277, 1134
Edelson, R.A., Malkan, M.A., 1986, ApJ, 308, 59
Gendron, E., et al., 1998, A&A research note, in preparation
Genzel, R., Weitzel, L., Tacconi-Garman, L.E., Blietz, M., Cameron, M., Krabbe, A., Lutz, D., Sternberg, A., 1995, ApJ, 444, 129
Glass, I., 1992, MNRAS, 256, 23P
Granato, G.L., Danese, L., 1994, MNRAS, 268, 235
Granato, G.L., Danese, L., Franceschini, A., 1996, ApJ, L11
Granato, G.L., Danese, L., Franceschini, A., 1997, ApJ, 147
Lacombe, F., Marco, O., Geoffray, H., et al., 1997, PASP, submitted
Marco, O., Alloin, D., Beuzit, J.L., 1997, A&A, 320, 399
Mazzarella, J.M., Voit, G.M., Soifer, B.T., Matthews, K., Graham, J.R., Armus, L., Shupe, D., 1994, AJ, 107 (4), 1274
Mauder, W., Weigelt, G., Appenzeller, I., Wagner, S.J., 1994, A&A, 285, 44
Miles, J.W., Houck, J.R., Hayward, T.L., Ashby, M.L.N., 1996, ApJ, 465, 191
Pier, E.A., Krolik, J.H., 1992a, ApJ, 399, L23
Pier, E.A., Krolik, J.H., 1992b, ApJ, 401, 99
Pier, E.A., Krolik, J.H., 1993, ApJ, 418, 673
Robson, E.I., et al., 1986, Nat, 323, 134
Sanders, D.B., Phinney, E.S., Neugebauer, G., et al., 1989, ApJ, 347, 29
Santos-Lléo, M., Clavel, J., Barr, P., Glass, I., Pelat, D., Peterson, B.M., Reichert, G., 1995, MNRAS, 274, 1
Wilson, A.S., Helfer, T.T., Haniff, C.A., Ward, M.J., 1991, ApJ, 381, 79